Forecasting the probability of the detection of a compact binary merger in a science run based on previous detections

Om Sharan Salafia[1,2]

[1] INAF – Osservatorio Astronomico di Brera, via Brera 28, I-20124 Milano (MI), Italy
e-mail: om.salafia@inaf.it
[2] INFN, Sezione di Milano-Bicocca, Piazza della Scienza 2, I-20126 Milano (MI), Italy

April 11, 2024

ABSTRACT

With no binary neutron star (BNS) merger detected during the first half of the fourth observing run (O4) of the LIGO-Virgo-KAGRA (LVK) network, despite a roughly doubled time-volume surveyed with respect to the end of O3, a pressing question is how likely the detection of at least one BNS merger is in the remainder second half of the run, due to start in a few months. I present here a simple and general method to address such a question, which constitutes the basis for the predictions to be presented in the LVK Public Alerts User Guide.

1. Poisson probability informed by previous occurrences of a rare event

The derivation here is essentially identical to that presented in Appendix B of Ray et al. (2023), and the result coincides with Eq. 42 in Essick (2023) in a particular case.

Let N be the a number of occurrences of a rare event over a period of time T, and let λ be the expected number of events, that is, the average occurrence rate multiplied by T. The probability of N given λ is the Poisson probability

$$p(N\,|\,\lambda) = \frac{\lambda^N \exp(-\lambda)}{N!}. \tag{1}$$

Now let N' be a number of previously observed events over a different time period T', over which the expected number of events was λ', with $C = \lambda/\lambda'$. The posterior probability on λ' given N' can be written through Bayes' theorem as

$$p(\lambda'\,|\,N') = \frac{p(N'\,|\,\lambda')\pi(\lambda')}{p(N')} = \frac{\lambda'^{N'}\exp(-\lambda')}{N'!}\frac{\pi(\lambda')}{p(N')}, \tag{2}$$

where $\pi(\lambda')$ is the prior probability on λ'. We opt to parametrize this as

$$\pi(\lambda') = \left(\frac{p(N')N'!}{\Gamma(N'+1-\alpha)}\right)\lambda^{-\alpha}, \tag{3}$$

where $\Gamma(x)$ is the Gamma function and the factor in parentheses ensures the correct normalization of the posterior. With this definition, $\alpha = 0$ corresponds to a uniform prior, $\alpha = 1/2$ to the Jeffreys prior for the Poisson probability, and $\alpha = 1$ to a uniform-in-logarithm prior.

These definitions allow us to derive the posterior probability on N given the previously observed number of events N', as follows. The starting point is

$$p(N\,|\,N') = \int p(N\,|\,\lambda)p(\lambda\,|\,N')\,\mathrm{d}\lambda = \\ = \int p(N\,|\,\lambda)\int p(\lambda\,|\,\lambda')p(\lambda'\,|\,N')\,\mathrm{d}\lambda'\,\mathrm{d}\lambda. \tag{4}$$

Noting that $p(\lambda\,|\,\lambda') = \delta(\lambda - C\lambda')$, where δ is the Dirac delta, this leads to

$$p(N\,|\,N') = \frac{C^{\alpha-N'-1}}{\Gamma(N'+1-\alpha)}\int p(N\,|\,\lambda)\exp\left(-\frac{\lambda}{C}\right)\lambda^{N'-\alpha}\,\mathrm{d}\lambda. \tag{5}$$

Substituting Eq. 1 in the above expression, carrying out the integral, and using $N! = \Gamma(N+1)$, we finally obtain

$$p(N\,|\,N',\alpha,C) = \frac{\Gamma(N+N'+1-\alpha)}{\Gamma(N+1)\Gamma(N'+1-\alpha)}\frac{C^N}{(1+C)^{N+N'+1-\alpha}}, \tag{6}$$

where the dependence on the prior index α and the expected number ratio C has been made explicit.

2. Application to compact binary mergers

For a gravitational wave detector network whose range does not extend to large redshifts, the cosmic evolution of the population and cosmological effects can be neglected, so that the expected number of detections over an observing run of duration T can be expressed simply as $\lambda = R_0 V T$, where R_0 is the local rate density of compact binary mergers and V is the effective volume over which the network is sensitive to such sources. In this context, the ratio λ/λ' is then simply the ratio of the effective sensitive time-volume of the run to that of past runs, namely

$$C = \frac{VT}{\sum_{l=1}^{n_\mathrm{past}} V_l T_l}, \tag{7}$$

where l runs over past observing runs. In the following, we describe a strategy to estimate such ratio using basic information such as the binary neutron star (BNS) ranges and duty cycles of the detectors.

2.1. Evaluation of the effective sensitive volume for each run

The 'optimal' matched filter signal-to-noise ratio (SNR) of a single merger ρ_opt, assuming that it is dominated by the inspiral part

of the signal, depends on the chirp mass $m_c = (m_1 m_2)^{3/5}/(m_1 + m_2)^{1/5}$ (where m_1 and m_2 are the gravitational masses of the primary and secondary components of the binary), the luminosity distance r, and on the detector noise power spectral density (PSD) curve $\mathcal{S}(f)$ as a function of frequency f through the integral[1] $f_{7/3} = \int \left[f^{7/3}\mathcal{S}(f)\right]^{-1} \mathrm{d}f$ (Finn & Chernoff 1993), so that

$$\rho_{\rm opt} \propto \frac{m_c^{5/6}}{r} f_{7/3}. \tag{8}$$

The actual SNR ρ in a given detector also depends on the source position in the detector's sky (defined e.g. by a pair of spherical angular coordinates θ, ϕ), its inclination ι with respect to the line of sight and its polarization angle ψ, all of which can be summarized into a single parameter $0 \leq w \leq 1$ such that $\rho = w\rho_{\rm opt}$ (Finn & Chernoff 1993; Dominik et al. 2015; Chen et al. 2021), with

$$w^2 = \frac{1}{4}F_+^2(\theta,\phi,\psi)(1+\cos^2\iota)^2 + F_\times^2(\theta,\phi,\psi)\cos^2\iota, \tag{9}$$

where F_+ and $F_\times$ are the 'antenna pattern' functions that define the dependence of the detector's sensitivity on sky position and polarization angle. The probability distribution of w for each detector is completely specified under the assumption of isotropic sky positions and binary orbital plane orientations. Since $w \leq 1$, and given the dependencies in Eq. 8, for each detector there exists a 'horizon' distance $d_{\rm h}(m_c) \propto m_c^{5/6} f_{7/3}$ such that $\rho_{\rm opt}(r = d_{\rm h}) = \rho_{\rm lim}$, where $\rho_{\rm lim}$ is a minimum SNR required for a detection. This represents the distance beyond which a binary with a chirp mass m_c cannot be detected. Hence, for a given binary, one can write the SNR in the i-th detector of a network as

$$\rho_i = w_i \rho_{\rm lim} \frac{d_{{\rm h},i}}{r}, \tag{10}$$

and the squared 'network SNR' in an n-detector network as

$$\rho_{\rm net}^2 = \sum_{i=0}^{n-1} \rho_i^2 = w_0^2 \rho_{\rm lim}^2 \frac{d_{\rm h,0}^2}{r^2}\left[1 + \sum_{i=1}^{n-1}\left(\frac{w_i}{w_0}\right)^2\left(\frac{d_{{\rm h},i}}{d_{\rm h,0}}\right)^2\right]. \tag{11}$$

For each detector, the ratio between the horizon distance $d_{{\rm h},i}$ and the BNS 'range' $\mathcal{R}$ is fixed (Chen et al. 2021), and hence $d_{{\rm h},i}/d_{\rm h,0} = \mathcal{R}_i/\mathcal{R}_0$.

Let us now represent the detection as a threshold on the network SNR $\rho_{\rm net} \geq \rho_{\rm lim}$. In other words, let us define the detection probability of a binary merger as

$$p_{\rm det} = \Theta\left(\rho_{\rm net} - \rho_{\rm lim}\right), \tag{12}$$

where Θ is the Heaviside step function. The effective sensitive volume of a network, neglecting cosmological effects, is then obtained by integrating the detection probability over volume and over the binary orientations,

$$V_{\rm eff} = \iiiii r^2 p_{\rm det} \mathrm{d}r \sin\theta\, \mathrm{d}\theta\, \mathrm{d}\phi \frac{\sin\iota\, \mathrm{d}\iota}{2}\frac{\mathrm{d}\psi}{2\pi} =$$
$$4\pi d_{\rm h,0}^3 \iiiii x^2 \Theta\left(\frac{\rho_{\rm net}}{\rho_{\rm lim}} - 1\right)\mathrm{d}x \frac{\sin\theta\,\mathrm{d}\theta}{2}\frac{\mathrm{d}\phi}{2\pi}\frac{\sin\iota\,\mathrm{d}\iota}{2}\frac{\mathrm{d}\psi}{2\pi} =$$
$$\frac{4\pi}{3} d_{\rm h,0}^3 \left\langle x_{\rm lim}^3 \right\rangle, \tag{13}$$

[1] We neglect here a small additional dependence on the component masses and possibly on the neutron star matter equation of state, which together determine the effective inspiral cut-off frequency.

where we defined the dimensionless distance $x = r/d_{\rm h,0}$ and its limiting value for detection at fixed sky position and inclination (which follows from Eq. 11)

$$x_{\rm lim}(\theta,\phi,\iota,\psi) = w_0(\theta,\phi,\psi)\left[1 + \sum_{i=1}^{n-1}\left(\frac{w_i(\tilde\theta_i,\tilde\phi_i,\iota,\tilde\psi_i)}{w_0(\theta,\phi,\iota,\psi)}\right)^2\left(\frac{\mathcal{R}_i}{\mathcal{R}_0}\right)^2\right]^{1/2}. \tag{14}$$

In the above expression, $(\tilde\theta_i, \tilde\phi_i)$ and $\tilde\psi_i$ represent the sky position and the polarization angle as seen by detector i, as opposed to (θ, ϕ) and ψ that pertain to the reference detector 0. The average $\langle x_{\rm lim}^3 \rangle$ is over isotropic sky positions and orientations. We call such average the 'geometrical factor' of the network. This is related to the 'peanut factor' $f_{\rm p}$ defined in Chen et al. (2021) through $f_{\rm p} = \langle x_{\rm lim}^3 \rangle^{-1/3}$. For $n = 1$, $\langle x_{\rm lim}^3 \rangle^{-1/3} = f_{\rm p} = 2.264$ is the usual horizon-to-range ratio (Finn & Chernoff 1993; Chen et al. 2021).

For each pair of detectors i and j, the probability distribution of the ratio

$$\frac{w_i}{w_j} = \frac{F_{+,i}^2(1+\cos^2\iota)^2 + 4F_{\times,i}^2\cos^2\iota}{F_{+,j}^2(1+\cos^2\iota)^2 + 4F_{\times,j}^2\cos^2\iota} \tag{15}$$

depends only on the relative orientations of the two detectors. Samples of such distribution can be obtained in a simple way by sampling isotropic sky positions and binary orientations, computing the antenna pattern functions of the two detectors for each sampled configuration, and constructing the ratio as expressed in the above equation. The resulting samples of the ratio can then be used to compute the geometrical factor $\langle x_{\rm lim}^3 \rangle$ with a Monte-Carlo sum. The horizon $d_{\rm h,0} = 2.264\mathcal{R}_0(m_c/m_{\rm c,ref})^{5/6}$, where $m_{\rm c,ref} = 1.22\,\mathrm{M}_\odot$ (Chen et al. 2021) is the reference chirp mass for which the BNS range is defined. These facts allows us to compute the effective sensitive volume of a network to a binary of chirp mass m_c by knowing only the detector orientations and their BNS ranges.

Since the duty cycle of the GW detectors is not 100%, at any time the GW detector network effectively acts as one of several possible sub-networks, depending on which combination of detectors is online. The formalism outlined above can be used to compute the effective sensitive volume of each of the sub-networks, and these can then be combined based on the fraction of time, in a given observing run, over which that particular sub-network was operating. From basic combinatorics, the number of sub-networks (i.e. possible combinations of online detectors) is

$$N_c(n) = \sum_{k=1}^{n} \binom{n}{k}, \tag{16}$$

where the sum is over n-choose-k Binomial coefficients. For a 3-detector network, this is $N_c(3) = 3 + 3 + 1 = 7$. For the HLV network, these seven combinations are H, L, V, HL, LV, VH, HLV. Let us number the observing runs of the GW detector network by an index l, and denote by n_l the number of detectors that participated in each run. If $f_{l,j}$ is the fraction of run l's time during which only the combination j of detectors was online (the others being offline or presenting data quality issues), then the total effective sensitive volume of the run is

$$V_l = \sum_{j=1}^{N_c(n_l)} f_{j,l} V_{{\rm eff},j,l} = \frac{4\pi}{3} d_{{\rm h},0,0,l}^3 \sum_{j=1}^{N_c(n_l)} f_{j,l}\left(\frac{\mathcal{R}_{0,j,l}}{\mathcal{R}_{0,0,l}}\right)^3 \left\langle x_{\rm lim}^3 \right\rangle_{j,l}, \tag{17}$$

Table 1. Run duration, representative BNS ranges of the detectors, and total effective sensitive time-volume to a BNS with $m_c = 1.22\,M_\odot$ of the past GW observing runs, and projections for O4b. The index l is included to ease the comparison with Eq. 17.

Index l	Run	Duration (days)	BNS range (Mpc)			$V_l T_l$ (10^{-3} Gpc^3 yr)
			H	L	V	
1	O1	130	70	60	–	0.43
2	O2	268	60	85	25	1.5
3	O3a	183	105	135	45	7.7
4	O3b	147	115	135	50	7.4
5	O4a	235	140	150	–	15
6	O4b	297	150	160	50	22

where $\mathcal{R}_{i,j,l}$ is the BNS range of i-th detector of combination j during run l, and similarly $d_{\mathrm{h},i,j,l}$ is the corresponding horizon distance.

We note that the ratio of effective sensitive volumes is independent of chirp mass, owing to the fact that the single-detector horizons (which are the only dimensional terms in Eq. 17) all share the same dependency $d_{\mathrm{h},0,0,l} \propto m_c^{5/6}$. This shows that the detection rate estimate based on Eq. 6 is insensitive to the mass distribution of the binaries of interest, as long as their SNR is reasonably well approximated by that of an inspiral of two point masses.

2.2. Application to BNS and NSBH mergers in O4b

Equation 17 allows us to write the ratio of expected numbers of BNS mergers C (Eq. 7) as a function of the BNS ranges of the detectors in each of the run (which we assume constant for simplicity), the durations of the runs, and the sub-network time fractions $f_{j,l}$. The durations of the runs and the representative BNS ranges of the detectors that we adopt here are reported in Table 1. These are based on the BNS range plots for each run and each detector as reported in the observing run summary pages of the public Gravitational Wave Open Science (GWOSC) website[2], and are representative values close to the peaks of the distributions of ranges reported there. For O4b, the projected ranges are based on the plots relative to the weeks preceding the start of O4b. In order to compute the sub-network time fractions, we retrieved the list of time segments that pass quality checks for the search of compact binary coalescences for each detector and each run from the GWOSC website[3]. This allowed us to extract the fraction of each run's time over which each sub-network was available. For O4b, we assumed the same fractions as O3b. The result is reported in Table 2, along with the geometrical factors computed using the ranges from Tab. 1.

Using the information in Table 2, we obtain $C = 0.87$. We note that, if we had evaluated this at the start of O4a, and we were interested in the ratio of the expected number of BNS merger detections in O4a to that of the previous runs, we would have obtained $C_{\mathrm{O4a}} \sim 0.85$. This implies that the absence of BNS merger detections in O4a decreases our estimate of the intrinsic BNS merger rate by a large factor, $1 + C_{\mathrm{O4a}} \sim 1.85$.

The left-hand panel in Fig. 1 shows with red squares the probability $p(N\,|\,N', \alpha, C)$ (Eq. 6) with $N' = 2$ and adopting the Jeffreys prior (i.e. setting $\alpha = 1/2$), for $C = 0.87$, hence referring to the number of BNS merger detections over O4b. The red squares in the right-hand panel show the probability of a number of BNS detections in O4b larger than, or equal to, the number on the horizontal axis. This shows that the most likely number is $N = 1$, and that the probability of at least one detection is around 73% assuming $\alpha = 1/2$. For $\alpha \in [0, 1]$, this probability varies in the range $71\% - 85\%$. Assuming the O3a duty cycles instead

Table 2. Fraction of past GW observing run time during which each sub-network was operational (i.e. was taking data that passes quality checks for the search of compact binary coalescences) and corresponding geometrical factor $\langle x_{\mathrm{lim}}^3 \rangle$ computed using the ranges from Tab. 1. The indices (j, l) are included to ease the comparison with Eq. 17.

Index (j,l)	Sub-network	Time fraction $f_{j,l}$	$\left\langle x_{\mathrm{lim}}^3 \right\rangle_{j,l}$
	O1		
(1,1)	H	0.21⋆	0.086
(2,1)	L	0.13⋆	0.086
(3,1)	HL	0.38	0.19
	O2		
(1,2)	H	0.14⋆	0.086
(2,2)	L	0.125⋆	0.086
(3,2)	V	0.0062⋆	0.086
(4,2)	HL	0.38	0.44
(5,2)	VH	0.0064	0.10
(6,2)	LV	0.0083	0.095
(2,2)	HLV	0.057	0.47
	O3a		
(1,3)	H	0.030	0.086
(2,3)	L	0.035	0.086
(3,3)	V	0.086	0.086
(4,3)	HL	0.14	0.36
(5,3)	VH	0.096	0.10
(6,3)	LV	0.14	0.097
(7,3)	HLV	0.44	0.39
	O3b		
(1,4)	H	0.031	0.086
(2,4)	L	0.023	0.086
(3,4)	V	0.064	0.086
(4,4)	HL	0.16	0.31
(5,4)	VH	0.10	0.11
(6,4)	LV	0.093	0.10
(7,4)	HLV	0.50	0.34
	O4a††		
(1,5)	H	0.15	0.086
(2,5)	L	0.15	0.086
(3,5)	HL	0.53	0.27
	O4b†††		
(1,6)	H	0.031	0.086
(2,6)	L	0.023	0.086
(3,6)	V	0.064	0.086
(4,6)	HL	0.16	0.26
(5,6)	VH	0.10	0.097
(6,6)	LV	0.093	0.096
(7,6)	HLV	0.50	0.28

†The KAGRA detector is not included for simplicity.
††Based on GWOSC detector status summary for O4a, because the data segments were not yet available at the time of writing.
†††Sub-network time fractions in O4b are set equal to those of O3b.
⋆These fractions are set to zero in the computation of the effective sensitive volume of the run, because single-detector triggers were not considered valid during these runs.

[2] https://gwosc.org/detector_status/
[3] https://gwosc.org/timeline/

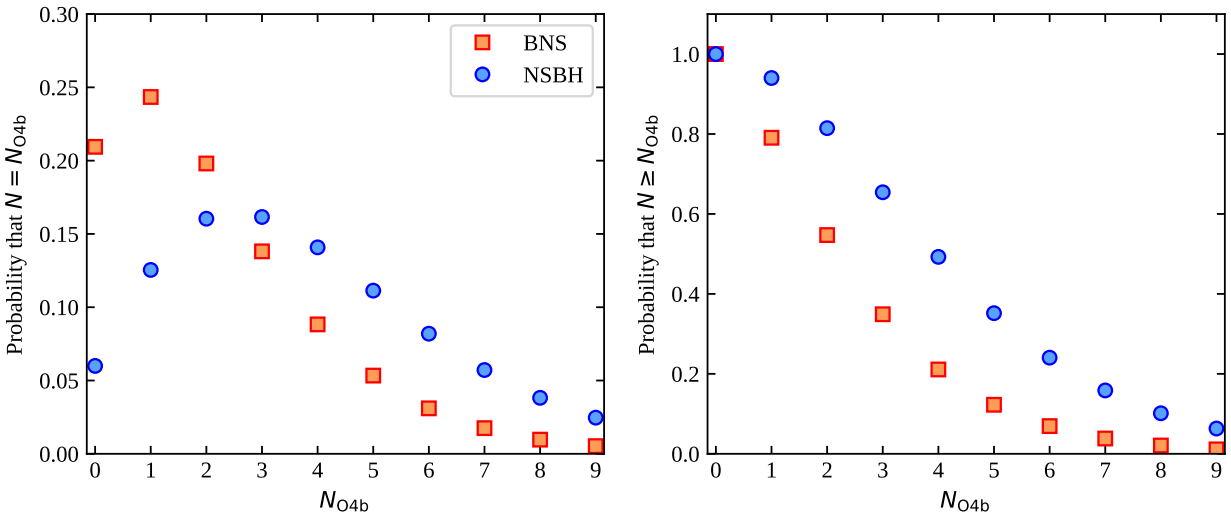

Fig. 1. BNS merger detection probability in O4b. The red squares in the left-hand panel show the probability that exactly N_{O4b} BNS mergers are detected by the LVK network during O4b, based on the number $N' = 2$ detected in previous runs, according to Eq. 6 and adopting the Jeffreys prior ($\alpha = 1/2$). The blue circles refer to NSBH instead, assuming $N' = 4$. In the right-hand panel, the probability of a number of detections $N \geq N_{O4b}$ in O4b is shown for the same two classes of sources.

of the O3b ones, decreases these probabilities by approsimately 2%.

The same approach can be applied to neutron star - black hole (NSBH) mergers, with the caveat that the inspiral-dominated signal approximation, and the fact that we neglect cosmological effects, can introduce some (small) systematic bias. Assuming $N' = 4$, which corresponds to the number of NSBH candidates with a false alarm rate (FAR)) lower than 1/4yr in the GWTC-3 catalog (Abbott et al. 2023) plus the two high-probability NSBH candidates released as public alerts up to the end of O4a, and again adopting the Jeffreys prior, we obtain the results shown by blue circles in Figure 1. Adopting different priors affects the resulting probability by a few percent.

At any time t after the start of O4b, we can also compute the probability of at least one detection in the remainder of the run (of duration $T - t$). This is obtained from

$$
\begin{aligned}
&p\left(N > 0 \,|\, N', \alpha, C(t)\right) = \\
&= 1 - p\left(N = 0 \,|\, N', \alpha, C = \left[\frac{1 - \frac{t}{T}}{C(0)\frac{t}{T} + 1}\right] C(0)\right) = \\
&= 1 - \left(\frac{C(0) + 1}{C(0)\frac{t}{T} + 1}\right)^{\alpha - 1 - N'} . \qquad (18)
\end{aligned}
$$

Solid lines in Fig. 2 show the resulting probability for three different prior choices, $\alpha = 0$, 1/2 and 1, keeping $N' = 2$. The grey dashed line shows the result for $\alpha = 1/2$ and $N' = 3$, which represents the updated probability estimate of at least an additional fourth detection in the remainder of O4 after a hypothetical third detection has been made.

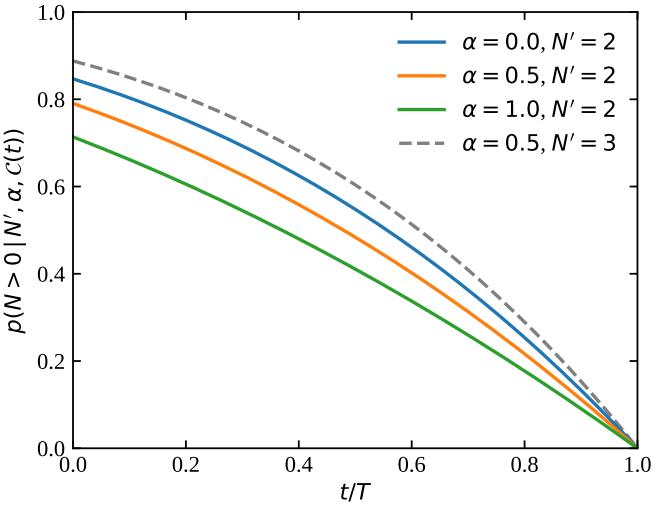

Fig. 2. Probability of at least one detection in the remainder of O4, as a function of time T from the start of O4b, for three different prior choices (different colours), keeping $N' = 2$ fixed (i.e. assuming no detection, solid lines). The dashed line represents the probability of at least one hypothetical further detection after a third detection has been made during O4b.

References

Abbott, R., Abbott, T. D., Acernese, F., et al. 2023, Physical Review X, 13, 041039

Chen, H.-Y., Holz, D. E., Miller, J., et al. 2021, Classical and Quantum Gravity, 38, 055010

Dominik, M., Berti, E., O'Shaughnessy, R., et al. 2015, ApJ, 806, 263

Essick, R. 2023, Physical Review D, 108, 043011

Finn, L. S. & Chernoff, D. F. 1993, Phys. Rev. D, 47, 2198

Ray, A., Camilo, M., Creighton, J., Ghosh, S., & Morisaki, S. 2023, Phys. Rev. D, 107, 043035